Journal of Physics: Theories and Applications E-ISSN: 2549-7324 / P-ISSN: 2549-7316
J. Phys.: Theor. Appl. Vol. 8 No. 1 (2024) 98-108 doi: 10.20961/jphystheor-appl.v8i1.86746

A Low-cost demonstration kit for determination of the active region of x-ray detectors using phototransistors.

Saminan[1], Fitria Silviana[2] and Soni Prayogi[3]*

[1]Department of Physics Education, Faculty of Teacher Training and Education, Syiah Kuala University, Banda Aceh 23111, Indonesia

[2]Department of Physics Education, Faculty of Mathematics and Natural Sciences, Medan State University, Medan 20221, Indonesia.

[3]Department of Electrical Engineering, Pertamina University, Jakarta 12220, Indonesia

E-mail: soni.prayogi@universitaspertamina.ac.id

Received 20 March 2024, Revised 23 March 2024, Published 30 March 2024

Abstract: This research develops a low-cost demonstration kit that aims to facilitate understanding of the concept of determining the active region of an X-ray detector using a phototransistor. This demonstration kit provides a practical and effective tool for illustrating the basic principles of X-ray detection, focusing on the phototransistor as the main component. The research method includes designing an electronic circuit capable of converting changes in light received by a phototransistor into an electrical signal that can be measured. The interaction of X-rays with matter can produce fluorescence phenomena that emit visible light. This phenomenon is utilized to design a phototransistor-based X-ray detector by attaching a ZnS (Ag) fluorescent screen to the surface of a phototransistor arranged in a Darlington circuit. The measurement of the active area of the detector was carried out by collimating the x-ray beam from a 2000-watt Philips x-ray generator tube, 60 kV type PW 2215/20 NR 780026, and measuring the output voltage of the detector (V_{out}) every 1 mm the change in beam position horizontally or vertically. The experimental results show that the Darlington circuit can be applied to design phototransistor-based X-ray detectors. The detector's active area irradiated with x-rays was obtained at (3.5 ± 0.5) mm horizontally and (3.3 ± 0.5) mm in the vertical direction. The results validate the phototransistor's response to X-rays and provide a clear illustration of how the active region of the detector can be identified and measured.

Keywords: Detector; Phototransistor; X-ray; Screen ZnS (Ag)..

1. Introduction

X-ray wavelengths and energies range from 0.01 nm to 10 nm, making them useful for medical diagnosis and therapy (Wang & Gu, 2022). CT scans measure the distribution of X-ray absorption coefficients, with the intensity measured by the detector. The number of detectors on a CT scan is determined by its generation (Nicholls et al., 2017). The first generation used parallel beam scanning, while the second generation had arrays facing a

single source (Marques et al., 2022). The third generation had detectors in concentric arcs, reducing data acquisition time (Bhowmik, 2011). The fourth generation had fixed sources and detectors mounted on rings, allowing for accurate distance measurements (Rambhujun et al., 2020). Gas-filled detectors, such as the Ionization Detector and Geiger Muller Detector (Chaiwongkhot et al., 2022), are commonly used but have large dimensions and low efficiency (Zhong et al., 2021). Semiconductor detectors offer advantages such as linear response (Prayogi, Cahyono, & Darminto, 2022), negligible energy absorption (Zhihong et al., 2022), excellent energy resolution (Prayogi et al., 2023), pulse formation (Scharenberg et al., 2022), fast rise time (Nagata et al., 2022), and small detector size (Prayogi, Asih, et al., 2022).

X-rays can ionize atoms in materials, causing fluorescence symptoms. A light detector is used to detect X-rays, such as a phototransistor made of p-n semiconductor material (Darminto et al., 2023). Phototransistors are more sensitive to changes in light, making them ideal for detecting X-rays (Manning et al., 2021). A fluorescent screen, such as Silver-Activated Zinc Sulfide (ZnS(Ag), is sensitive to x-rays and can emit high-frequency electromagnetic waves (Costa & Muleri, 2014). The detector can measure the output in current or voltage. To digitize the output, an ADC (*Analog to Digital Converter*) is used to convert the analog signal into a digital value (Hamdani et al., 2022). A smaller 3 mm phototransistor is used in this study, as it has a higher sensitivity compared to a photodiode and can be used as an X-ray detector in CT scans. The study aims to determine the active region of the phototransistor near the ZnS(Ag) fluorescent screen, which could potentially be applied to X-ray detectors in Computed Tomography (CT) scans.

This study focuses on precise dose evaluation using a commercial phototransistor as a radiation detector for X-ray doses in the diagnostic range (Benali et al., 2022). The circuit is designed to change the electric field within the phototransistor (Hu et al., 2022), allowing for a response from a specified range of photon energies (Yadav et al., 2021). The method is tested using a radiation beam from the Pantak HF-160 X-ray unit and compared to the usual dosimetry method (Scisciò et al., 2022).

2. Experimental Method

The research was conducted at the Pertamina University Physics Laboratory, Jakarta. The materials needed are ZnS (Ag) as a fluorescent screen, a 2N2369 transistor, and a 3 mm phototransistor. The equipment used includes an x-ray generator from a Shimadzu XD-300 XRD tool complete with a generator transformer and a Shimadzu CWK-3500 cooling system. A 2000-watt, 60 kV Philips x-ray generator tube with PW type 2215/20 NR.780026. Surveimeter, 10-bit Analog to Digital Converter found on Arduino UNO R3, and Computer (PC) functions to write programs and display analog data results which are converted into digital form using ADC. The circuit used in the study is shown in Figure 1.

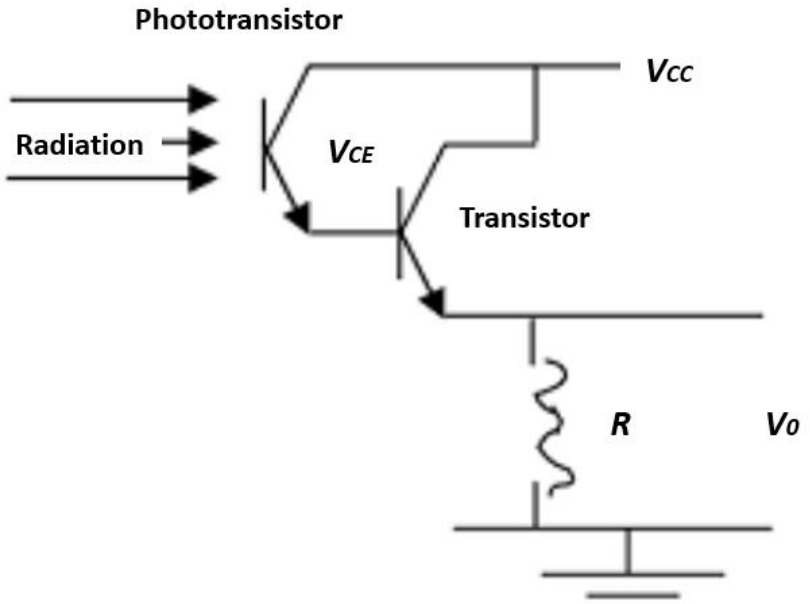

Figure 1. The schematic darlington Type Circuit.

This circuit is used to design a phototransistor detector that is brought closer to the ZnS (Ag) fluorescent screen to detect x-rays with an output in the form of a voltage (V_{out}) which is then connected to the ADC to convert analog values into digital values. The designed detector consists of a ZnS (Ag) fluorescent screen which is placed close to the face of the phototransistor (Prayogi et al., 2019). This detector then measures the active area horizontally and vertically by scanning it using a single X-ray beam (pencil beam). The voltage and current of the filament in the X-ray generator are kept constant and the position of the detector changes by 1 mm for each scan. The output of the detector in the form of voltage (V_{out}) is measured and displayed on a computer screen (PC), as illustrated in Figure 2.

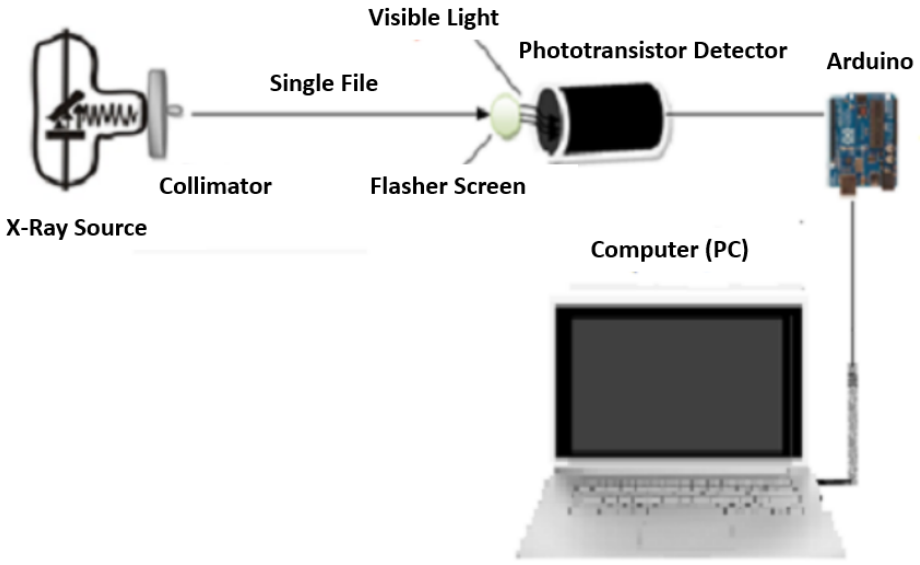

Figure 2. Illustration of measuring the active area of an X-ray detector.

3. Results and Discussion

Data from the experimental results of the active area of the detector horizontally are shown in Table 1 and vertically shown in Table 2. Table 1 explains that the lowest value is (114.3 ± 0.2) mV at the 0 mm position, while the highest value is (417.8 ± 3) mV at the 8 mm position, that is, in the mid-range. These results are then plotted in the form of a graph of the relationship between the distance between the horizontal detector faces and the value of the output voltage at the detector shown in Figure 3.

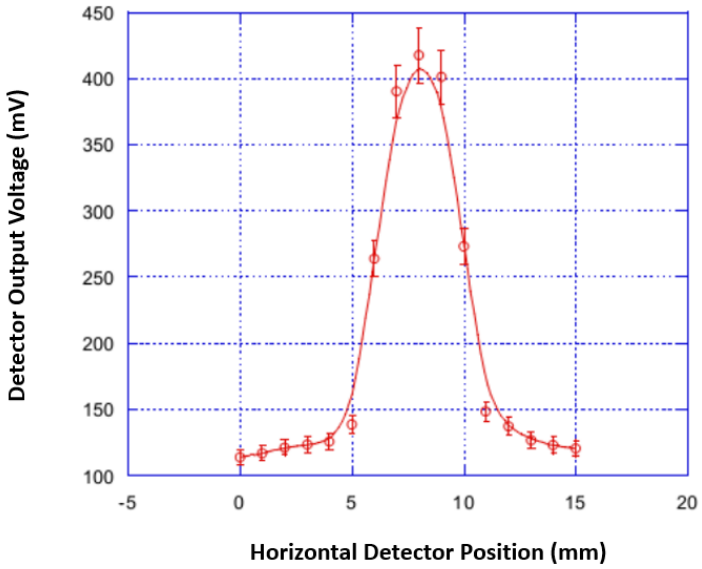

Figure 3. The relationship between the beam position (mm) and the detector output (mV) in the horizontal direction

Table 1. Results of measuring the active area of the detector horizontally.

Number	X-Ray Beam Position (mm)	Detector Output Voltage (mV)
1	0	114.3 ± 0.2
2	1	117.2 ± 0.2
3	2	121.6± 0.2
4	3	123.7 ± 0.5
5	4	125.8 ± 0.2
6	5	138.7 ± 0.2
7	6	264.3 ± 0.2
8	7	390.3 ± 1
9	8	417.8 ± 3
10	9	401.5 ± 5
11	10	273.4 ± 4
12	11	148.8 ± 1
13	12	137.4 ± 1
14	13	127.1 ± 0.3
15	14	123.2 ± 0.3
16	15	120.8 ± 2

Figure 3 shows the relationship between the detector position (mm) and the detector output voltage (mV) horizontally, explaining that the experimental results are normally distributed. The FWHM (Full Width at Half Maximum) value is 3.5 mm, this value describes the active area of the phototransistor detector after the ZnS (Ag) fluorescent screen is brought closer to the horizontal direction, namely (3.5 ± 0.5) mm. The ZnS (Ag) fluorescent screen plays an important role in the detector (Prayogi et al., 2017), namely when the detector that has been installed with a fluorescent screen interacts with x-rays it will produce fluorescence phenomena which produce visible light in the range of violet light (Prayogi et al., 2021).

Table 2 is the result of measuring the active area of the phototransistor detector vertically, measurements are made repeatedly to get better measurement results. The x-ray beam that hits the detector area is collimated so that the resulting x-ray is in the form of a single beam (pencil beam), this is done so that the measured detector output voltage is correct from the area (point) being tested by 1 mm. The lowest value is (112.7 ± 0.3) mV at the 0 mm position and the highest value is at the 8 mm position, namely (397.6 ± 12.7) mV. These results are then plotted in the form of a relationship between the position of the detector and the output voltage of the phototransistor detector, shown in Figure 4.

Figure 4 shows the relationship between the position of the detector (mm) and the output voltage of the vertical direction of the phototransistor detector (mV) that has been developed. The experimental data were normally distributed with the highest value (397.6 ± 12.7) mV. From Figure 5.4, we get a variance of 1.42 so the FWHM value obtained is (3.3 ± 0.5) mm, which is the active region of the vertical phototransistor detector. The diameter of the phototransistor (3 ± 0.25) mm which is brought closer to the ZnS (Ag) fluorescent screen with a thickness of 1 mm can produce a large enough output voltage from mV to V (Naseer et al., 2022). The active region is along the diameter of the detector and the response of the detector is linear when irradiated with X-rays it is a hope of success if this detector is applied to detect x-rays, especially in the CT-scan field which requires many detector arrays (Rattyananda et al., 2022). However, testing the detector's response to X-rays still needs to be done by constructing a detector array consisting of several phototransistors (Schreiner et al., 2009). To implement a phototransistor detector as a detector array (Neubüser et al., 2022), it is necessary to test the detector's response to x-rays that have passed through materials with different homogeneity so that in the end it is expected that phototransistors can be applied to the CT-scan field (Nazhmudinov et al., 2022).

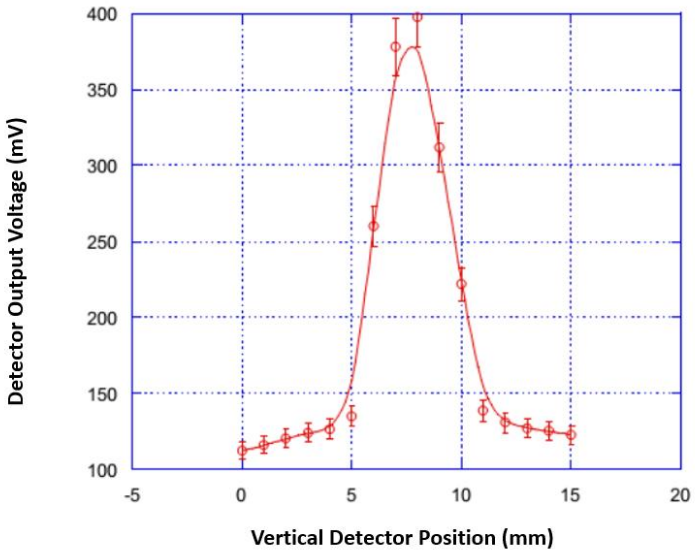

Figure 4. Relationship between beam position (mm) and Detector Output (mV) in the vertical direction.

Table 2. Results of measuring the active area of the detector vertically.

Number	X-Ray Beam Position (mm)	Detector Output Voltage (mV)
1	0	112.7 ± 0.3
2	1	116.1 ± 0.2
3	2	120.5 ± 0.6
4	3	124.1 ± 0.1
5	4	126.5 ± 1.4
6	5	134.9 ± 0.3
7	6	260.1 ± 0.6
8	7	378.1 ± 0.4
9	8	397.6 ± 12.7
10	9	312.0 ± 0.4
11	10	222.1 ± 0.5
12	11	138.7 ± 0.2
13	12	131.1 ± 0.2
14	13	127.2 ± 2
15	14	125.4 ± 0.3
16	15	122.8 ± 0.5

The low-cost demonstration kit developed in this research successfully illustrates the concept of X-ray detection using phototransistors. In these results it was also found that Phototransistor Response Validation: The calibration experiment succeeded in validating the phototransistor response to X-rays. The results show that phototransistors can convert changes in X-ray intensity into electrical signals that can be measured well (Prayogi, Cahyono, Hamdani, et al., 2022). Detector Active Region Illustration: This demonstration kit is effective in illustrating how the active region of an X-ray detector can be identified and measured (Beavers et al., 2022). This demonstration allows users to see changes in

phototransistor response with changes in position or X-ray intensity. Educational Use: This kit has great potential in teaching and understanding X-ray detection concepts. In an educational context, this kit can be used as a tool to educate students about the basic principles in X-ray detection. Potential Use in Research: This demonstration kit also has potential in scientific research. Users working in related fields can use this kit to illustrate or validate basic principles in their experiments (Dong et al., 2022).

This research makes an important contribution to the development of a low-cost demonstration kit for X-ray detection using phototransistors. This kit can help educate and increase understanding of X-ray detection technology (Arratia et al., 2022), both in educational and scientific research contexts. This kit also allows greater accessibility to this understanding, given its low cost. However, there are several considerations that need to be considered. First, in the context of the use of X-ray sources, radiation safety is very important (Choi et al., 2022). Users of this kit must comply with all applicable rules and regulations regarding the use of X-rays. Second, the kit needs to be adapted to the type of X-ray detector used in the experiment (D'Andrea et al., 2022). Finally, further research could develop this kit by adding additional features or more complex options for a deeper understanding.

4. Conclusion

In summary, the phototransistor detector which is approached by the ZnS (Ag) fluorescent screen has an active area of (3.5 ± 0.5) mm in the horizontal direction and (3.3 ± 0.5) mm in the vertical direction and can produce a large enough output voltage of mV to V. The designed detector can detect X-rays with good capabilities. This research succeeded in developing a low-cost demonstration kit for determining the active region of an X-ray detector using a phototransistor. This kit is effective in illustrating the basic principles in X-ray detection and can be used in education as well as scientific research. The development of such kits is important to increase understanding of X-ray detection technology and make it more accessible to a wide range of audiences. This kit also has the potential for further development with more advanced features according to user needs.

Acknowledgments

The author also acknowledges your use of experimental resources at Pertamina University and Medan State University.

References

Arratia, M., Butter, A., Campanelli, M., Croft, V., Gillberg, D., Ghosh, A., Lohwasser, K., Malaescu, B., Mikuni, V., Nachman, B., Rojo, J., Thaler, J., & Winterhalder, R. (2022). Publishing unbinned differential cross section results. *Journal of Instrumentation*, *17*(01), P01024. https://doi.org/10.1088/1748-0221/17/01/P01024

Beavers, J., Huddleston, K., Hines, N., & McNeil, W. (2022). Modeling electron transport and multiplication in photomultiplier tubes using COMSOL Multiphysics®.

Journal of Instrumentation, *17*(12), P12015. https://doi.org/10.1088/1748-0221/17/12/P12015

Benali, A., Ishak-Boushaki, G. M., Riffaud, J., & Nourreddine, A.-M. (2022). Geometrical effects on luminescent dosimeter energy response. *Journal of Instrumentation*, *17*(01), P01035. https://doi.org/10.1088/1748-0221/17/01/P01035

Bhowmik, S. (2011). Effect of Radiation and Vacuum. In L. F. M. da Silva, A. Öchsner, & R. D. Adams (Eds.), *Handbook of Adhesion Technology* (pp. 823–844). Springer. https://doi.org/10.1007/978-3-642-01169-6_32

Chaiwongkhot, K., Kin, T., Nagata, Y., Komori, T., Okamoto, N., & Basiri, H. (2022). 3D cosmic-ray muon tomography using portable muography detector. *Journal of Instrumentation*, *17*(01), P01009. https://doi.org/10.1088/1748-0221/17/01/P01009

Choi, H., Ko, K., Kim, W., Lee, J., Sun, G., Chang, H., Yi, Y., & Cho, G. (2022). Study of timing performance parameters for a SiPM-based digital positron annihilation lifetime spectrometer. *Journal of Instrumentation*, *17*(12), C12007. https://doi.org/10.1088/1748-0221/17/12/C12007

Costa, E., & Muleri, F. (2014). Gamma and X-Radiation. In E. G. Njoku (Ed.), *Encyclopedia of Remote Sensing* (pp. 219–228). Springer. https://doi.org/10.1007/978-0-387-36699-9_49

D'Andrea, V., Biondi, R., Ferrari, C., Ferella, A. D., Mahlstedt, J., & Pieramico, G. (2022). The ABALONE photosensor. *Journal of Instrumentation*, *17*(01), C01038. https://doi.org/10.1088/1748-0221/17/01/C01038

Darminto, D., Asih, R., Priyanto, B., Baqiya, M. A., Ardiani, I. S., Nadiyah, K., Laila, A. Z., Prayogi, S., Tunmee, S., Nakajima, H., Fauzi, A. D., Naradipa, M. A., Diao, C., & Rusydi, A. (2023). Unrevealing tunable resonant excitons and correlated plasmons and their coupling in new amorphous carbon-like for highly efficient photovoltaic devices. *Scientific Reports*, *13*(1), Article 1. https://doi.org/10.1038/s41598-023-31552-5

Dong, J., Pan, Z., Lin, Z., Wang, Z., He, Z., Liu, J., Zhang, H., Jing, H., Bao, Y., Tang, J., & Ye, B. (2022). Optimization of detector placements in reduction of multiple counts for μSR measurements at China Spallation Neutron Source. *Journal of Instrumentation*, *17*(01), P01017. https://doi.org/10.1088/1748-0221/17/01/P01017

Hamdani, D., Prayogi, S., Cahyono, Y., Yudoyono, G., & Darminto, D. (2022). The Effects of Dopant Concentration on the Performances of the a-SiOx:H(p)/a-Si:H(i1)/a-Si:H(i2)/μc-Si:H(n) Heterojunction Solar Cell. *International Journal of Renewable Energy Development*, *11*(1), 173–181. https://doi.org/10.14710/ijred.2022.40193

Hu, Q., Ye, H. Q., Zhang, Q. L., Yi, G. H., Chen, L., Xu, X. Y., & Jin, G. (2022). Handheld portable neutron gamma discrimination spectrometer for environmental detection. *Journal of Instrumentation*, *17*(12), T12002. https://doi.org/10.1088/1748-0221/17/12/T12002

Manning, B. R., Ashton, J. P., & Lenahan, P. M. (2021). Observation of electrically

detected electron nuclear double resonance in amorphous hydrogenated silicon films. *Applied Physics Letters*, *118*(8), 082401. https://doi.org/10.1063/5.0041059

Marques, L., Félix, L., Cruz, G., Coelho, V., Caetano, J., Vale, A., Cruz, C., Alves, L., & Vaz, P. (2022). Neutron and Gamma-Ray Detection System Coupled to a Multirotor for Screening of Shipping Container Cargo. *Sensors (Basel, Switzerland)*, *23*(1), 329. https://doi.org/10.3390/s23010329

Nagata, J., Yamamoto, S., Noguchi, Y., Nakaya, T., Okudaira, K., Kamada, K., & Yoshikawa, A. (2022). Erratum: Development of a simultaneous imaging system to measure the optical and gamma ray images of Ir-192 source for high-dose-rate brachytherapy. *Journal of Instrumentation*, *17*(01), E01001. https://doi.org/10.1088/1748-0221/17/01/E01001

Naseer, A. P., Krishna, U. S., & Unni, P. K. M. (2022). High-precision thermostat for light scattering experiments of critical samples. *Journal of Instrumentation*, *17*(12), P12007. https://doi.org/10.1088/1748-0221/17/12/P12007

Nazhmudinov, R. M., Shchagin, A. V., Kubankin, A. S., Afonin, A. G., Britvich, G. I., Durum, A. A., Kostin, M. Y., Maisheev, V. A., Pitalev, V. I., Chesnokov, Y. A., & Yanovich, A. A. (2022). Measurement of ionization loss of 50 GeV protons in silicon with smoothly tunable up to 1 cm thickness using a single flat detector. *Journal of Instrumentation*, *17*(01), P01015. https://doi.org/10.1088/1748-0221/17/01/P01015

Neubüser, C., Corradino, T., Mattiazzo, S., Pancheri, L., & collaboration, on behalf of the A. (2022). Impact of X-ray induced radiation damage on FD-MAPS of the ARCADIA project. *Journal of Instrumentation*, *17*(01), C01035. https://doi.org/10.1088/1748-0221/17/01/C01035

Nicholls, D. C., Dopita, M. A., Sutherland, R. S., & Kewley, L. J. (2017). Chapter 17—Electron Kappa Distributions in Astrophysical Nebulae. In G. Livadiotis (Ed.), *Kappa Distributions* (pp. 633–655). Elsevier. https://doi.org/10.1016/B978-0-12-804638-8.00017-6

Prayogi, S., Asih, R., Priyanto, B., Baqiya, M. A., Naradipa, M. A., Cahyono, Y., Darminto, & Rusydi, A. (2022). Observation of resonant exciton and correlated plasmon yielding correlated plexciton in amorphous silicon with various hydrogen content. *Scientific Reports*, *12*(1), Article 1. https://doi.org/10.1038/s41598-022-24713-5

Prayogi, S., Ayunis, A., Cahyono, Y., & Darminto, D. (2023). N-type H2-doped amorphous silicon layer for solar-cell application. *Materials for Renewable and Sustainable Energy*. https://doi.org/10.1007/s40243-023-00232-9

Prayogi, S., Ayunis, Kresna, Cahyono, Y., Akidah, & Darminto. (2017). Analysis of thin layer optical properties of A-Si:H P-Type doping CH4 and P-Type without CH4 is deposited PECVD systems. *Journal of Physics: Conference Series*, *853*(1), 012032. https://doi.org/10.1088/1742-6596/853/1/012032

Prayogi, S., Baqiya, M. A., Cahyono, Y., & Darminto. (2019). Optical Transmission of p-Type a-Si:H Thin Film Deposited by PECVD on ITO-Coated Glass. *Materials Science Forum*, *966*, 72–76. https://doi.org/10.4028/www.scientific.net/MSF.966.72

Prayogi, S., Cahyono, Y., & Darminto, D. (2022). Electronic structure analysis of a-Si: H p-i1-i2-n solar cells using ellipsometry spectroscopy. *Optical and Quantum Electronics*, *54*(11), 732. https://doi.org/10.1007/s11082-022-04044-5

Prayogi, S., Cahyono, Y., Hamdani, D., & Darminto. (2022). Effect of active layer thickness on the performance of amorphous hydrogenated silicon solar cells. *Engineering and Applied Science Research*, *49*(2), Article 2.

Prayogi, S., Cahyono, Y., Iqballudin, I., Stchakovsky, M., & Darminto, D. (2021). The effect of adding an active layer to the structure of a-Si: H solar cells on the efficiency using RF-PECVD. *Journal of Materials Science: Materials in Electronics*, *32*(6), 7609–7618. https://doi.org/10.1007/s10854-021-05477-6

Rambhujun, N., Salman, M. S., Wang, T., Pratthana, C., Sapkota, P., Costalin, M., Lai, Q., & Aguey-Zinsou, K.-F. (2020). Renewable hydrogen for the chemical industry. *MRS Energy & Sustainability*, *7*(1), 33. https://doi.org/10.1557/mre.2020.33

Rattyananda, B. S., Martoprawiro, M. A., Arifah, A., Meliawati, A. P., Widayanti, M. I., Tursinah, R., & Setiadi, Y. (2022). Computation Study of Radioisotopes Gallium-68 (68Ga) Production using Long-lived & High Activity methods. *Jurnal Sains Dan Teknologi Nuklir Indonesia (Indonesian Journal of Nuclear Science and Technology)*, *22*(2), Article 2. https://doi.org/10.17146/jstni.2021.22.2.6440

Scharenberg, L., Bortfeldt, J., Brunbauer, F., Christensen, M. J., Desch, K., Flöthner, K., Garcia, F., Janssens, D., Kaminski, J., Lisowska, M., Lupberger, M., Muller, H., Oliveri, E., Orlandini, G., Pfeiffer, D., Ropelewski, L., Rusu, A., Samarati, J., Schwäbig, P., … Veenhof, R. (2022). Development of a high-rate scalable readout system for gaseous detectors. *Journal of Instrumentation*, *17*(12), C12014. https://doi.org/10.1088/1748-0221/17/12/C12014

Schreiner, L. J., Joshi, C. P., Darko, J., Kerr, A., Salomons, G., & Dhanesar, S. (2009). The role of Cobalt-60 in modern radiation therapy: Dose delivery and image guidance. *Journal of Medical Physics / Association of Medical Physicists of India*, *34*(3), 133–136. https://doi.org/10.4103/0971-6203.54846

Scisciò, M., Consoli, F., Salvadori, M., Rosmej, O. N., Zähter, S., Giorgio, G. D., Andreoli, P. L., Cipriani, M., Cristofari, G., Angelis, R. D., Günther, M. M., Gyrdymov, M., & Tavana, P. (2022). High sensitivity Thomson spectrometry: Analysis of measurements in high power picosecond laser experiments. *Journal of Instrumentation*, *17*(01), C01055. https://doi.org/10.1088/1748-0221/17/01/C01055

Wang, C., & Gu, C. (2022). X-Ray Diffraction. In *Reference Module in Earth Systems and Environmental Sciences*. Elsevier. https://doi.org/10.1016/B978-0-12-822974-3.00037-9

Yadav, S., Singh, O. P., Choudhary, S., Saroj, D. K., Yogi, V., & Goswami, B. (2021). Estimation and comparison of integral dose to target and organs at risk in three-dimensional computed tomography image-based treatment planning of carcinoma uterine cervix with two high-dose-rate brachytherapy sources: 60: Co and: 192: Ir. *Journal of Cancer Research and Therapeutics*, *17*(1), 191. https://doi.org/10.4103/jcrt.JCRT_199_19

Zhihong, Z., Shimazoe, K., & Takahashi, H. (2022). Characterization of time-of-flight double-photon Compton imaging system by simulation. *Journal of Instrumentation*, *17*(01), C01045. https://doi.org/10.1088/1748-0221/17/01/C01045

Zhong, Z., Wang, X., Yin, X., Tian, J., & Komatsu, S. (2021). Morphophysiological and Proteomic Responses on Plants of Irradiation with Electromagnetic Waves. *International Journal of Molecular Sciences*, *22*(22), Article 22. https://doi.org/10.3390/ijms222212239